Crystal Structure and Spectroscopic Studies of the Complexes $[HgX(NO_3)(PPh_3)]$ (X = Cl, Br or I)†

Lisa-Jane Baker,[a] Graham A. Bowmaker,*[,a] Peter C. Healy,[b] Brian W. Skelton[c] and Allan H. White[c]

[a] *Department of Chemistry, University of Auckland, Private Bag 92019, Auckland, New Zealand*

[b] *Division of Science and Technology, Griffith University, Nathan, Queensland 4111, Australia*

[c] *Department of Physical and Inorganic Chemistry, University of Western Australia, Nedlands, W.A. 6009, Australia*

The structures of the complexes $[HgX(NO_3)(PPh_3)]$ (X = Cl, Br or I) have been determined by single-crystal X-ray diffraction. All three crystallize in the monoclinic space group $P2_1/c$ with one formula unit comprising the asymmetric unit of the structure. Their structures are quite similar, but that of the chloride differs in a number of respects from those of the bromide and iodide, which are isostructural. In each complex the mercury atom environment is dominated by close associations with the halide and phosphorus atoms in a quasi-linear array, but significant deviations from linearity arise, presumably because of contacts normal to the P–Hg–X array by the nitrate oxygens [Hg–X 2.328(2), 2.4386(8) and 2.601(1); Hg–P 2.372(1), 2.388(1) and 2.402(2) Å; P–Hg–X 158.44(6), 166.05(4) and 166.17(5)° for X = Cl, Br and I respectively]. The nitrate moieties link successive mercury atoms in a one-dimensional polymeric array. In all three structures one of the Hg • • • O contacts, designated O(1), is shorter [2.527(5), 2.594(6) and 2.586(7) Å respectively] than those to the other two oxygen atoms which lie at 2.7–2.9 Å. In the bromide and iodide complexes both of these are to O(2), which bridges adjacent mercury atoms; in the chloride the nitrate bridges to an adjacent mercury atom by way of a bidentate O(2,3) interaction. These structural features are reflected in the infrared spectra in the ν(HgX) and nitrate ν(NO) regions. Raman measurements yield assignments for ν(HgP) in the range 147–164 cm^{-1}. The solution ^{31}P NMR spectra in MeCN show that $[HgX(NO_3)(PPh_3)]$ is the only species in solution for X = Cl, but for X = Br or I a partial symmetrization to $[Hg(NO_3)_2(PPh_3)_2]$ and HgX_2 occurs. The ^{31}P cross polarization magic angle spinning (CP MAS) NMR spectra of the solids exhibit a single line due to species which contain non-magnetic isotopes of mercury, in agreement with the existence of only one molecule in the asymmetric unit, and satellite lines due to $^1J(^{199}Hg^{31}P)$ coupling. Broader satellites which can be shown to be due to the presence of scalar spin–spin coupling between ^{31}P and the quadrupolar ^{201}Hg nucleus ($I = \frac{3}{2}$, natural abundance = 13.22%) are also observed. This agrees well with the predicted form of the spectrum of a spin $\frac{1}{2}$ nucleus coupled to a spin $\frac{3}{2}$ nucleus for the case of a small dipolar coupling interaction between the nuclei and a large nuclear quadrupole interaction at the $I = \frac{3}{2}$ nucleus. The ^{31}P NMR parameters measured for $[HgX(NO_3)(PPh_3)]$ in the solid state are compared with those observed for the corresponding complexes in MeCN solution. The chemical shifts are not strongly dependent on X, but the variation with X is in opposite directions for the solution and solid samples. The $^1J(^{199}Hg^{31}P)$ values show opposite trends for the chloride (increasing from the solution to the solid state) relative to the bromide and iodide complexes (where a decrease is observed). This may be related to the difference in the crystal structures of the complexes.

Complexes of the type [HgX(Y)L] (L = tertiary phosphine or arsine; X = Cl, Br or I; Y = NO_3 or BF_4) have been known for some time.[1–3] Infrared, NMR and NQR studies suggested that they contain $[HgX(L)]^+$ cations with only weakly interacting Y^- anions. This was supported in the case of the BF_4^- complexes by the observation that their solutions in nitromethane showed conductivities appropriate for 1:1 electrolytes.[3] The nitrate complexes, however, are poor conductors in nitromethane solution, suggesting that the nitrate ion is co-ordinated to some extent.[3] The closely related complex $[HgPh(NO_3)(PPh_3)]$ consists essentially of $[HgPh(PPh_3)]^+$ and NO_3^- ions, with a weak interaction between the mercury and the nitrate oxygen atoms which results in a P–Hg–C(Ph) angle of 167.5(2)° instead of the 180° expected for the isolated cation.[4]

In the present study the structures of $[HgX(NO_3)(PPh_3)]$ (X = Cl, Br or I) have been determined by single-crystal X-ray diffraction methods. The infrared spectra of these complexes have been remeasured, and the results interpreted in terms of the structural data. The Raman spectra have also been measured in order to determine the ν(HgP) wavenumbers. The ^{31}P cross polarization magic angle spinning (CP MAS) NMR spectra were recorded and compared with the solution spectra in order to investigate the relationship between the structures of these complexes in the solid state and in solution. On the basis of the expectation that the complexes would contain $[HgX(PPh_3)]^+$ ions, which are isoelectronic with $[AuX(PPh_3)]$, another aim of the CP MAS NMR measurements was to try to obtain further information on the reason for the unexpected splittings which have been observed in the ^{31}P CP MAS NMR spectra of $[AuX(PPh_3)]$.[5]

† *Supplementary data available:* see Instructions for Authors, *J. Chem. Soc., Dalton Trans.*, 1992, Issue 1, pp. xx–xxv.

Experimental

Preparation of Compounds.—The compounds $[HgX(NO_3)(PPh_3)]$ (X = Cl, Br or I) were prepared by a previously described method which involves the reaction between $[Hg(NO_3)_2(PPh_3)_2]$ and HgX_2,[3] and also by the following new method. To a hot, stirred suspension of $[HgX_2(PPh_3)_2]$ (1.0 mmol) in ethanol (20 cm^3) was added a solution of $Hg(NO_3)_2 \cdot H_2O$ (0.34 g, 1 mmol) in water (2 cm^3) and concentrated HNO_3 (1 cm^3). The products separated immediately as white, microcrystalline solids which were collected by vacuum filtration, washed with ethanol (10 cm^3) and air-dried. The IR spectra of these products were identical to those prepared by the previously described method.[3]

Structure Determinations.—Slow crystallization of the complexes from absolute ethanol by solvent evaporation yielded well formed crystals suitable for X-ray structure determination.

Unique data sets were measured at ≈295 K within the limit $2\theta_{max} = 60°$ using an Enraf–Nonius CAD-4 diffractometer (monochromatic Mo-Kα radiation, $\lambda = 0.7107_3$ Å; 2θ–θ scan mode) yielding N independent reflections, N_o with $I > 3\sigma(I)$ being considered 'observed' and used in the full-matrix least-squares refinement after solution of the structures by the heavy-atom method (all structures are monoclinic, space group $P2_1/c$ (C_{2h}^5, no. 14), $Z = 4$; the bromide and iodide are isomorphous). Analytical absorption corrections were applied. Anisotropic thermal parameters were refined for the non-hydrogen atoms; $(x, y, z, U_{iso})_H$ were included constrained at estimated values. Conventional residuals R,R' on $|F|$ are quoted at convergence; statistical weights derivative of $\sigma^2(I) = \sigma^2(I_{diff}) + 0.0004\sigma^4(I_{diff})$ were used. Neutral atom complex scattering factors were employed,[6] computation using the XTAL 3.0 program system.[7] Pertinent results are shown in Figs. 1 and 2 and in Tables 1–3.

Crystal and refinement data for $[HgX(NO_3)(PPh_3)]$ (= $C_{18}H_{15}XHgNO_3P$). X = Cl, $M = 560.3$, $a = 9.803(4)$, $b = 9.940(6)$, $c = 19.312(5)$ Å, $\beta = 95.97(2)°$, $U = 1872$ Å^3, $D_c = 1.99$ g cm^{-3}, $F(000) = 1064$, $\mu_{Mo} = 81$ cm^{-1}, specimen 0.43 × 0.21 × 0.41 mm, $A^*_{min,max} = 3.26, 7.64$, $N = 5438$, $N_o = 3879$; $R = 0.034$, $R' = 0.036$.

X = Br, $M = 604.8$, $a = 9.514(3)$, $b = 18.655(3)$, $c = 11.085(2)$ Å, $\beta = 110.14(2)°$, $U = 1847$ Å^3, $D_c = 2.17$ g cm^{-3}, $F(000) = 1136$, $\mu_{Mo} = 102$ cm^{-1}, specimen 0.22 × 0.32 × 0.60 mm, $A^*_{min,max} = 3.46, 8.01$, $N = 5081$, $N_o = 3595$, $R = 0.033$, $R' = 0.034$.

X = I, $M = 651.8$, $a = 9.609(4)$, $b = 18.688(8)$, $c = 11.181(9)$ Å, $\beta = 109.19(5)°$, $U = 1894$ Å^3, $D_c = 2.29$ g cm^{-3}, $F(000) = 1208$, $\mu_{Mo} = 95$ cm^{-1}, specimen 0.15 × 0.28 × 0.40 mm, $A^*_{min,max} = 3.18, 7.74$, $N = 5426$, $N_o = 3870$, $R = 0.038$, $R' = 0.039$.

Additional material available from the Cambridge Crystallographic Data Centre comprises H-atom coordinates, thermal parameters and remaining bond lengths and angles.

Spectroscopy.—Infrared spectra were recorded at 4 cm^{-1} resolution at room temperature as pressed KBr discs on a Digilab FTS-60 Fourier-transform spectrometer employing an uncooled DTGS detector, far-infrared spectra at 4 cm^{-1} resolution at room temperature as pressed polythene discs on the same spectrometer employing an FTS-60V vacuum optical bench with a 6.25 μm mylar-film beam splitter, a mercury-lamp source and a TGS detector. Raman spectra were excited with 100 mW of radiation (514.5 nm) using a Coherent model 52 argon-ion laser, and were recorded at 4.5 cm^{-1} resolution using a Jobin-Yvon U1000 spectrometer. Solution $^{31}P-\{^1H\}$ NMR spectra were obtained at room temperature on a Bruker AM-400 spectrometer at a frequency of 161.98 MHz. Chemical shifts were referenced to 85% H_3PO_4 *via* trimethyl phosphite (δ = 139.2). The ^{31}P CP MAS NMR spectra were obtained at room temperature on a Bruker CXP-300 spectrometer at a frequency of 121.47 MHz, and on a Varian Unity 400 spectrometer at a frequency of 161.90 MHz. Spinning rates of *ca.* 3 kHz were used. Chemical shifts were referenced to 85% H_3PO *via* solid triphenylphosphine (δ = −9.9).

Results and Discussion

X-Ray Structure Determinations.—All three complexes crystallize in the monoclinic space group $P2_1/c$ with one formula unit comprising the asymmetric unit of the structure. The structures are quite similar but also subtly and interestingly different: the bromide and iodide are isostructural in a cell with a long b axis, but the chloride cell is related by an interchange of b and c (Fig. 1). As a consequence, the polymer arising from the concatenation of successive asymmetric units and lying parallel to the shorter axis of the bc plane is generated in the chloride by a 2_1 screw axis, but in the bromide and iodide by a glide plane. The chirality of successive mercury atom environments in any given polymer strand is therefore preserved in the chloride, but alternates in the bromide and iodide (Fig. 2). In each complex the mercury atom environment is dominated by close associations with the halide and phosphorus atoms in a quasi-linear array (Table 2), but significant deviations from linearity arise from contacts normal to the P–Hg–X array by the nitrate oxygens so that the description of the system in terms of a $[HgX(PPh_3)]^+[NO_3]^-$ cation–anion array is an oversimplification. The nitrate moieties bridge successive mercury atoms to form polymeric chain structures, but the mode of bridging differs in the two polymer types: in all three structures one of the Hg···O contacts, designated O(1), is shorter (at 2.5–2.6 Å) than those to the other two oxygen atoms which lie at 2.7–2.9 Å. In the bromide and iodide complexes both of these are to O(2), which itself performs the bridging function between adjacent mercury atoms; in the chloride, the nitrate bridges to an adjacent mercury atom by way of a bidentate O(2,3) interaction, *i.e.* as shown.

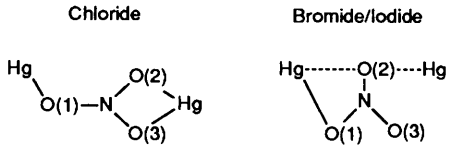

Deviations of the mercury atoms from the nitrate planes are given in Table 3; the nitrate groups themselves are not significantly distorted from planarity. At a lower level of significance, the oxygen atom O(3), which has the least interaction with the mercury, has the shortest N–O distance (Table 3), while the bidentate angle in the bromide and iodide, but not the chloride, is diminished below 120°. About the mercury, the halide X is terminal rather than bridging; Hg–X increases with X as expected, and there is a greater proportional increase relative to Hg–X in gas-phase HgX_2[8] in the case of the chloride (2.1%) than in the bromide (1.6%) or the iodide (1.2%). This suggests that the acceptor properties of HgX^+ decrease from X = Cl to I, and this is supported by the observation of a small increase in Hg–P along the series. The bond length Hg–I in $[HgI(NO_3)(PPh_3)]$ is only slightly shorter than the value of 2.62 Å in $[(HgI)_2TiF_6]$, which contains a zigzag array of HgI^+ linked by bridging through the iodine atoms, with nearly linear I–Hg–I.[9]

Comparison of the present results with those for $[HgPh(NO_3)(PPh_3)]$[4] reveals that Hg–P is significantly shorter for X = Cl, Br or I (2.37–2.40 Å) than for X = Ph (2.43 Å). This is consistent with the greater *trans* influence of the phenyl relative to the halide ligands.[10] Nevertheless, the P–Hg–C(Ph) angle [167.5(2)°] shows a degree of distortion from linearity which is similar to that of the P–Hg–X angles in the present complexes (particularly for the X = Br or I cases).

The Hg–X and Hg–P bond lengths in the present complexes are compared in Table 4 with those of 1:1 and 2:1 adducts of PPh_3 with HgX_2. The 1:1 adducts are dimers $[\{HgX_2(PPh_3)\}_2]$

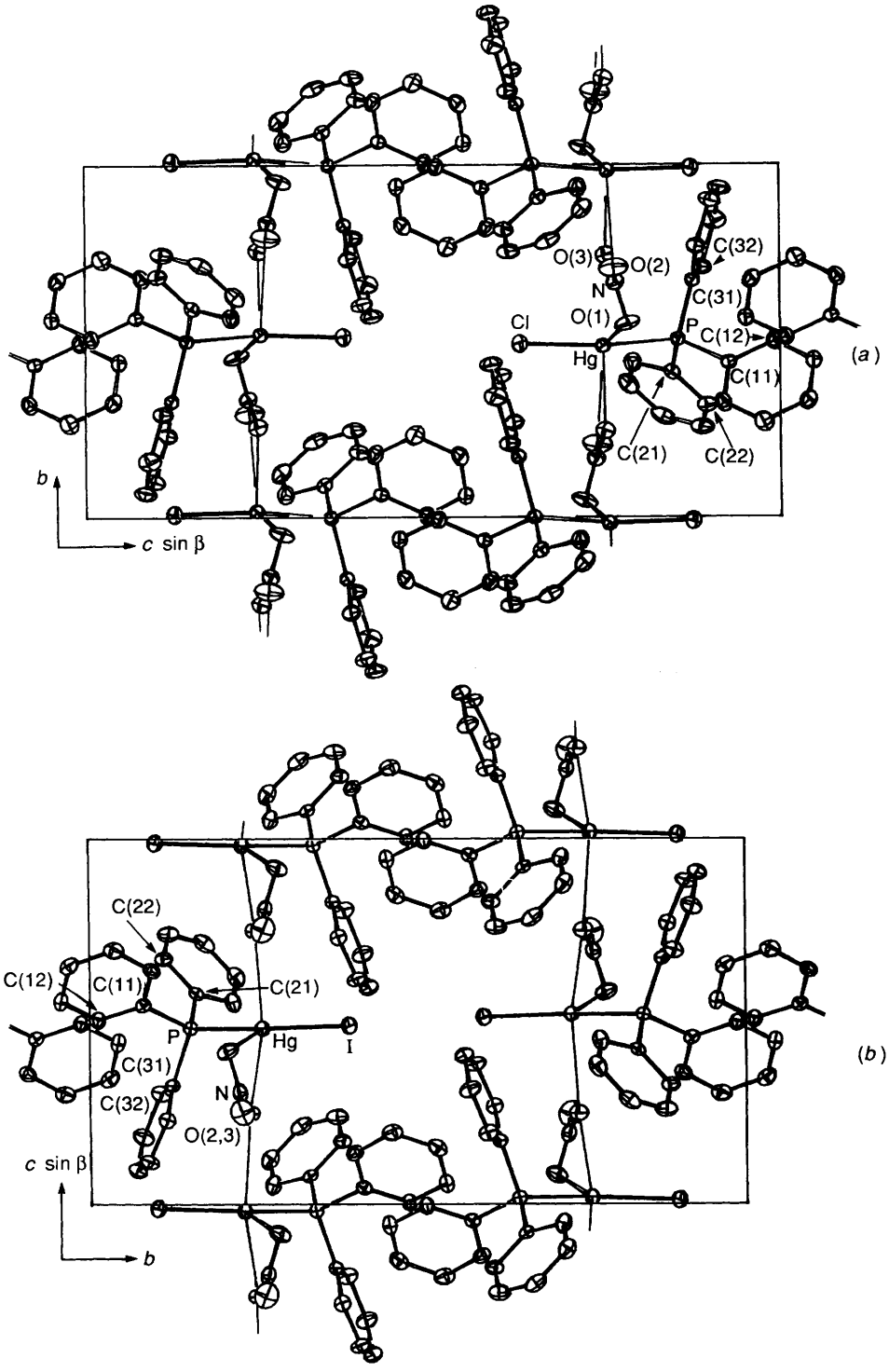

Fig. 1 Unit-cell contents, projected down *a*, of (*a*) $[HgCl(NO_3)(PPh_3)]$ and (*b*) $[HgI(NO_3)(PPh_3)]$; 20% thermal ellipsoids are shown for the non-hydrogen atoms. Both axis systems are right-handed

with two bridging halides linking the two mercury atoms, and a terminal halogen atom and PPh_3 molecule on each mercury atom,[11,12] while the 2:1 adducts are monomeric with two terminal halogen atoms and two PPh_3 molecules bound to the Hg atom in a pseudo-tetrahedral arrangement.[13,14] The terminal Hg–X bond lengths and the Hg–P bond lengths undergo a marked decrease in the transition from $[HgX_2(PPh_3)_2]$ to $[\{HgX_2(PPh_3)\}_2]$, and this is mainly a consequence of the removal of one PPh_3 molecule from the mercury co-ordination sphere. There is a further decrease in these parameters in the transition from $[\{HgX_2(PPh_3)\}_2]$ to $[HgX(NO_3)(PPh_3)]$, and this is a consequence of the replacement of the halide bridges in the former by the more weakly co-ordinated nitrate ion in the latter. This is also reflected in an increase in the P–Hg–X angle involving the terminal halide (Table 4).

Vibrational Spectra.—The far-infrared spectra of the three compounds reported are shown in Fig. 3. These show sharp, intense, halogen-sensitive bands at 321, 231 and 189 cm^{-1} (X = Cl, Br or I) which can readily be assigned as ν(Hg–X) modes. In the case of the chloride complex this band has a

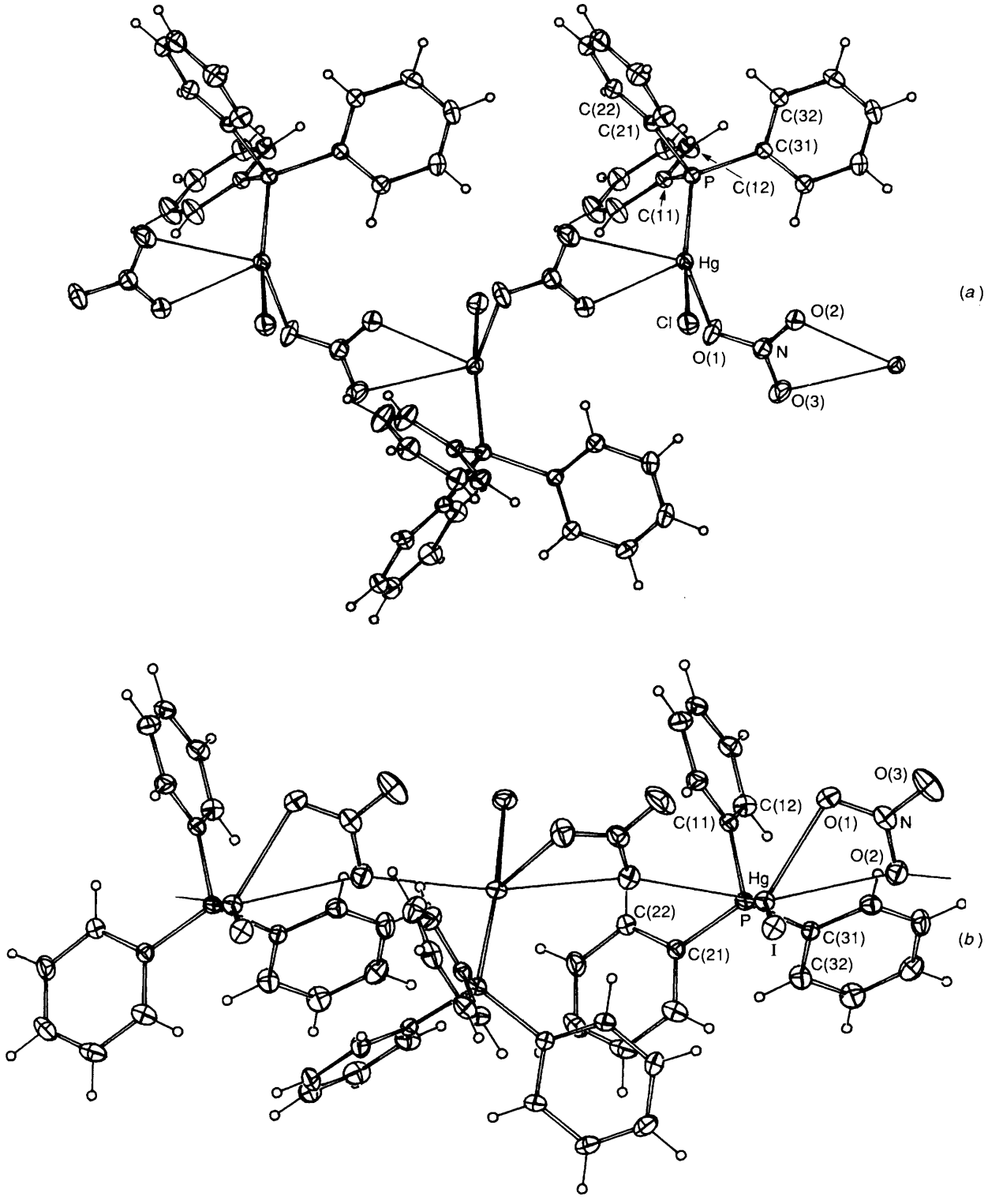

Fig. 2 The polymers of $[HgX(NO_3)(PPh_3)]$ [X = Cl(*a*) or I(*b*)] projected normal to the chain axis

shoulder at 315 cm^{-1} which can be assigned to the heavier chlorine isotope, ^{37}Cl.[17] Assignments of the ν(Hg–X) wavenumbers for these and for some related PPh_3 complexes of mercury(II) halides are given in Table 4. The present assignments are supported by the monotonic increase in ν(HgX) with decreasing Hg–X bond length which is observed for the compounds listed. Such a relationship has been observed previously for a wide range of mercury halide complexes, and the present results fit in very well with the correlations reported there.[18]

The Raman spectra in the range 100–450 cm^{-1} are shown in Fig. 4. These spectra show ν(HgX) bands at 319, 230 and 187 cm^{-1} (X = Cl, Br or I) which are almost exactly the same as the wavenumbers of the corresponding bands in the far-IR spectra. The intensities of the ν(HgX) bands decrease in the IR but increase in the Raman from X = Cl to I. This is a consequence of the decrease in ionic character and concomitant increase in covalent character of the Hg–X bonds along this series, as has been shown more directly from the halogen nuclear quadrupole

Table 1 Non-hydrogen atom coordinates in $[HgX(NO_3)(PPh_3)]$

	X = Cl			X = Br			X = I		
Atom	*x*	*y*	*z*	*x*	*y*	*z*	*x*	*y*	*z*
Hg	0.149 96(2)	0.483 02(2)	0.746 47(1)	0.208 85(3)	0.736 32(1)	0.514 44(2)	0.200 24(3)	0.735 25(1)	0.518 94(3)
X	0.089 3(2)	0.489 9(2)	0.626 71(8)	0.133 58(9)	0.611 01(3)	0.507 79(7)	0.114 51(6)	0.602 65(3)	0.511 14(5)
P	0.290 7(1)	0.501 0(1)	0.853 67(6)	0.336 1(2)	0.846 82(7)	0.515 4(1)	0.330 5(2)	0.844 96(9)	0.518 1(2)
C(11)	0.211 3(5)	0.434 6(5)	0.926 4(2)	0.207 0(6)	0.918 5(3)	0.451 1(5)	0.204 3(7)	0.917 8(3)	0.454 9(6)
C(12)	0.236 3(6)	0.493 8(6)	0.991 6(3)	0.237 1(6)	0.987 5(3)	0.500 6(5)	0.241 4(8)	0.986 9(4)	0.495 0(7)
C(13)	0.181 6(7)	0.438 5(7)	1.048 5(3)	0.142 4(8)	1.043 7(3)	0.443 8(7)	0.150 1(9)	1.044 0(4)	0.443 5(8)
C(14)	0.102 2(7)	0.326 4(7)	1.040 5(3)	0.020 7(8)	1.032 3(4)	0.336 7(7)	0.023(1)	1.030 9(4)	0.345 5(8)
C(15)	0.077 2(8)	0.267 3(7)	0.976 2(3)	−0.012 0(8)	0.964 3(4)	0.286 0(7)	−0.017 7(9)	0.962 0(5)	0.303 1(8)
C(16)	0.130 2(7)	0.321 3(7)	0.918 6(3)	0.081 0(8)	0.907 5(3)	0.342 8(6)	0.074 5(9)	0.904 5(4)	0.359 3(7)
C(21)	0.445 3(5)	0.407 5(5)	0.845 3(3)	0.454 0(6)	0.838 1(3)	0.419 0(5)	0.449 3(7)	0.836 0(3)	0.422 4(6)
C(22)	0.494 8(6)	0.315 4(6)	0.895 0(3)	0.447 4(7)	0.888 1(3)	0.323 8(6)	0.441 3(9)	0.885 6(4)	0.326 9(7)
C(23)	0.623 5(7)	0.254 0(7)	0.888 1(4)	0.543 6(8)	0.882 5(4)	0.254 2(6)	0.538 6(9)	0.878 6(5)	0.259 4(7)
C(24)	0.690 8(7)	0.283 6(7)	0.832 4(4)	0.641 5(8)	0.826 6(4)	0.276 4(7)	0.638 4(9)	0.823 3(5)	0.284 6(8)
C(25)	0.641 7(7)	0.374 0(8)	0.783 0(4)	0.649 4(8)	0.777 1(3)	0.370 6(7)	0.645 9(9)	0.775 1(4)	0.376 8(9)
C(26)	0.518 3(7)	0.435 2(7)	0.788 9(3)	0.553 2(8)	0.781 8(3)	0.440 2(7)	0.550 1(9)	0.779 8(4)	0.447 3(8)
C(31)	0.340 8(5)	0.671 7(5)	0.875 3(2)	0.453 9(6)	0.875 5(3)	0.673 6(5)	0.445 7(7)	0.873 6(3)	0.673 6(6)
C(32)	0.478 3(7)	0.708 6(6)	0.887 9(3)	0.603 4(7)	0.891 5(3)	0.700 6(6)	0.592 6(8)	0.891 4(4)	0.695 6(7)
C(33)	0.512 3(8)	0.839 5(8)	0.907 5(4)	0.687 6(8)	0.918 0(4)	0.820 2(7)	0.675 2(9)	0.918 7(5)	0.814 7(8)
C(34)	0.410 6(9)	0.931 9(7)	0.914 5(4)	0.624 3(8)	0.928 0(4)	0.912 7(6)	0.613(1)	0.927 8(4)	0.907 1(7)
C(35)	0.277 7(8)	0.897 6(6)	0.900 6(3)	0.474 4(8)	0.910 5(3)	0.886 8(6)	0.467(1)	0.909 6(4)	0.884 0(7)
C(36)	0.240 5(6)	0.767 6(6)	0.880 8(3)	0.390 7(7)	0.884 1(3)	0.768 3(6)	0.385 8(8)	0.882 0(4)	0.769 0(7)
N	−0.111 6(6)	0.666 2(5)	0.764 5(2)	0.022 8(7)	0.769 2(3)	0.687 6(6)	0.017 0(8)	0.769 7(3)	0.693 2(7)
O(1)	−0.082 5(5)	0.547 3(5)	0.718 6(3)	−0.013 2(6)	0.787 3(3)	0.572 9(5)	−0.015 2(7)	0.788 6(3)	0.580 5(6)
O(2)	−0.019 1(4)	0.744 1(4)	0.750 7(2)	0.156 2(6)	0.754 6(2)	0.746 4(4)	0.147 5(7)	0.754 2(3)	0.750 3(5)
O(3)	−0.231 5(5)	0.706 7(5)	0.762 3(3)	−0.068 1(7)	0.766 9(3)	0.744 0(7)	−0.075 1(9)	0.766 5(4)	0.747 6(8)

Table 2 The mercury environments (distances in Å, angles in °) in $[HgX(NO_3)(PPh_3)]$

	X = Cl	X = Br	X = I
Hg–X	2.328(2)	2.4386(8)	2.601(1)
Hg–P	2.372(1)	2.388(1)	2.402(2)
Hg–O(1)	2.527(5)	2.594(6)	2.586(7)
Hg–O(2′)	2.703(4)	2.843(5)	2.884(6)
Hg–O(*n*)	2.870(5)	2.804(5)	2.816(7)
X–Hg–P	158.44(6)	166.05(4)	166.17(5)
X–Hg–O(1)	96.6(1)	95.9(1)	95.9(1)
X–Hg–O(2′)	88.48(9)	94.66(9)	94.9(1)
X–Hg–O(*n*)	90.8(1)	90.06(9)	90.0(1)
P–Hg–O(1)	101.8(1)	97.9(1)	97.9(1)
P–Hg–O(2′)	106.40(9)	82.0(1)	81.4(1)
P–Hg–O(*n*)	89.0(1)	98.1(1)	98.5(1)
O(1)–Hg–O(2′)	76.9(1)	111.9(2)	111.6(2)
O(1)–Hg–O(*n*)	121.5(1)	46.2(1)	46.0(2)
O(2′)–Hg–O(*n*)	45.3(1)	158.1(1)	157.6(2)
Hg–O(1)–N	110.8(4)	101.2(4)	101.9(5)
Hg–O(2′)–N′	100.6(3)	108.4(5)	108.8(4)
Hg–O(*n*)–N	92.5(4)	91.1(4)	90.8(5)
Hg–O(2)–Hg′	—	160.5(2)	160.4(3)

For *n* read 3′ for the chloride, 2 for the bromide and iodide; primed atoms are generated by $x, \frac{3}{2} - y, z - \frac{1}{2}$ (bromide, iodide) or $x, y - \frac{1}{2}, \frac{3}{2} - z$ (chloride).

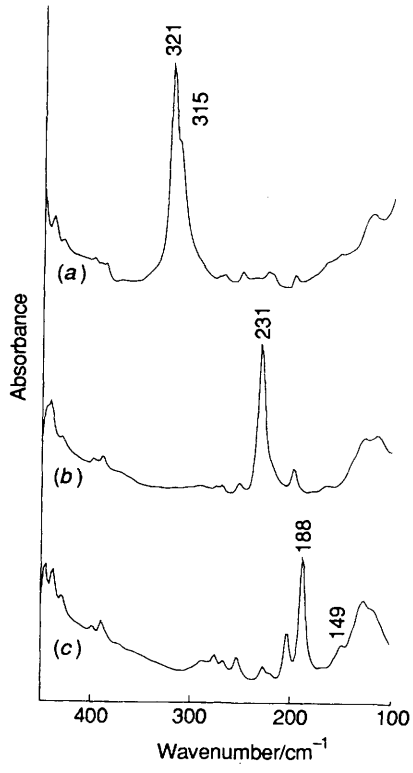

Fig. 3 Far-infrared spectra of $[HgX(NO_3)(PPh_3)]$ [X = Cl (*a*), Br (*b*) or I (*c*)]. Bands due to ν(HgX) and ν(HgP) are labelled with their wavenumbers

resonance frequencies in the case of the X = Cl and Br complexes.[3]

There have been a number of reported assignments of ν(HgP) bands in the vibrational spectra of complexes of mercury(II) halides with tertiary phosphines,[15,16,19] and some of these are listed in Table 4. If a monotonic relationship between ν(HgP) and the Hg–P bond length exists, then the bond lengths found in the present study for $[HgX(NO_3)(PPh_3)]$ imply ν(HgP) wavenumbers in the range 160–170 cm^{-1}. There are no strong bands present in the far-IR spectra in this region (Fig. 3) which could be definitely assigned to such modes. However, the Raman spectra (Fig. 4) show strong bands at 164, 161 and 147 cm^{-1}. Comparison with the Raman spectra of $[AuX(PPh_3)]$, in which strong bands at 182 and 173 cm^{-1} (X = Cl or Br) have been assigned as ν(AuP),[20] suggests that these are due to ν(HgP). The increase in the intensity of this band from X = Cl to I is probably a consequence of the fact that, as ν(HgX) decreases, the degree of mixing of ν(HgX) and ν(HgP) increases,

so that ν(HgP) gains some of the intensity associated with ν(HgX). This mixing is greatest for the X = I case, where the frequencies of the two bands are closest, and this results in the intensities of both bands being considerably greater than those of the co-ordinated PPh_3 molecule in the same region. Another consequence of this mixing for the X = I case is the fact that the predominantly ν(HgP) mode appears as a weak band at 149 cm^{-1} in the IR spectrum.

It was noted above that the nitrate ion in $[HgX(NO_3)(PPh_3)]$ is distorted from D_{3h} symmetry to a greater extent in the X = Br or I complexes than in the X = Cl case. This difference is evident in the IR spectra of these complexes. The distortion from D_{3h} symmetry which occurs upon co-ordination of the nitrate ion results in a lifting of the degeneracy of the E′ vibrational modes of this ion.[21–23] The vibration which is most sensitive to this distortion is ν_3 (the E′ N–O stretching mode), which occurs at 1390 cm^{-1} in the IR spectrum of unco-ordinated nitrate.[21] Splitting of ν_3 occurs in all three complexes, and the band positions and splittings are listed in Table 5. In the bromide and iodide complexes the higher-wavenumber component of this split band is further split, and the total splitting is greater in these than in the chloride complex, in agreement with the relative degrees of distortion found in the crystal structures.

Solution ^{31}P *NMR Spectra.*—These spectra were obtained by using MeCN as solvent. The spectrum of the chloride showed a single central line due to species which contain the non-magnetic isotopes of Hg, together with satellites which are assigned to $^1J(^{199}Hg^{31}P)$ coupling (^{199}Hg, 16.84% natural abundance, nuclear spin $I = \frac{1}{2}$). Similar lines assignable to $[HgX(NO_3)(PPh_3)]$ species were observed in the spectra of the bromide and iodide complexes, and the $\delta(^{31}P)$ and $^1J(^{199}Hg^{31}P)$ values are given in Table 6. In the case of the bromide and iodide complexes, however, there was a signal due to an additional species with $\delta(^{31}P)$ 46.2, $^1J(^{199}Hg^{31}P) = 5910$ Hz which was stronger in the iodide compared with the bromide case. This signal was shown to be due to $[Hg(NO_3)_2(PPh_3)_2]$ by recording the spectrum of this complex separately in MeCN. This result indicates the presence of a symmetrization equilibrium (1) in solution. This equilibrium lies entirely to the

$$2[HgX(NO_3)(PPh_3)] \rightleftharpoons [Hg(NO_3)_2(PPh_3)_2] + HgX_2 \quad (1)$$

left for X = Cl, but shifts significantly to the right for X = Br or I. However, the unsymmetrical species on the left-hand side is predominant in all three cases.

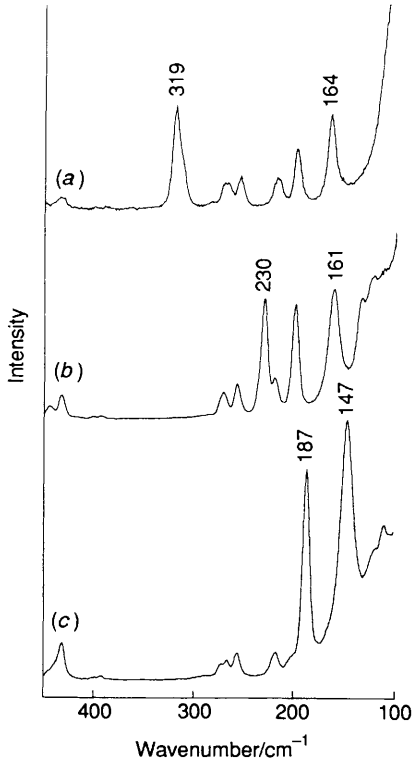

Fig. 4 Low-wavenumber Raman spectra of $[HgX(NO_3)(PPh_3)]$ [X = Cl (*a*), Br (*b*) or I (*c*)]. Bands due to ν(HgX) and ν(HgP) are labelled with their wavenumbers

Table 3 Nitrate geometries (distances in Å, angles in °) in $[HgX(NO_3)(PPh_3)]$

	X = Cl	X = Br	X = I
N–O(1)	1.252(7)	1.244(8)	1.244(9)
N–O(2)	1.243(7)	1.241(8)	1.240(9)
N–O(3)	1.239(8)	1.230(11)	1.229(13)
O(1)–N–O(2)	119.6(5)	117.9(7)	117.4(8)
O(1)–N–O(3)	120.3(5)	122.3(6)	122.4(7)
O(2)–N–O(3)	120.1(5)	119.7(6)	120.3(7)
Mercury deviations (Å) from the NO_3 plane			
Hg	−0.70(1)	−0.84(1)	−0.91(1)
Hg′	0.63(1)	0.87(1)	0.96(1)

Hg′ is related to Hg by $\bar{x}, \frac{1}{2} + y, \frac{3}{2} - z$ (X = Cl), or $x, \frac{3}{2} - y, \frac{1}{2} + z$ (Br, I).

Table 4 Structural (bond lengths in Å, angles in °) and vibrational parameters [absorption wavenumbers (cm^{-1}); X_t = terminal halide] for $[HgX(NO_3)(PPh_3)]$ and some related mercury halide complexes

Complex	X	Hg–X_t	Hg–P	P–Hg–X_t	ν(HgX_t)	ν(HgP)	Refs.
$[HgX(NO_3)PPh_3)]$	Cl	2.328(2)	2.372(1)	158.44(6)	321	164	*a*
	Br	2.4386(8)	2.388(1)	166.05(4)	231	161	*a*
	I	2.601(1)	2.402(2)	166.17(5)	189	147	*a*
$[\{HgX_2(PPh_3)\}_2]$	Cl	2.370(10)	2.406(7)	128.7(4)	291	157	11, 15
					288		
	Br				203	137[b]	15
					190		
	I	2.671(2)	2.461(8)	128.4(2)	163	139[b]	12, 15
		2.684(2)	2.483(8)	126.6(2)	139		
$[HgX_2(PPh_3)_2]$	Cl	2.545(3)	2.462(2)	99–109	232	137	13, 16
		2.559(2)	2.478(2)		221	108	
	Br	2.626(8)	2.535(15)		153	132	13, 16
		2.633(6)	2.540(16)			104	
	I	2.733(1)	2.557(3)		127	133	14, 16
		2.763(1)	2.574(3)			98	

[a] This work. [b] Assignment uncertain [assigned bands are coincident with ν(HgX) bands].

Table 5 Nitrate ν_3 band positions and splittings (cm^{-1}) for $[HgX(NO_3)(PPh_3)]$

X	Wavenumber			Splitting
Cl	1292	1381		89
Br	1288	1379	1398	110
I	1287	1379	1398	111

Table 6 Solution (MeCN) and solid-state ^{31}P NMR parameters for $[HgX(NO_3)(PPh_3)]$

	δ		$^1J(^{199}Hg^{31}P)$/Hz	
X	Solution	Solid	Solution	Solid
Cl	42.3	30.5	7980	8085
Br	42.2	32.2	7700	7400
I	41.1	33.0	6800	6330

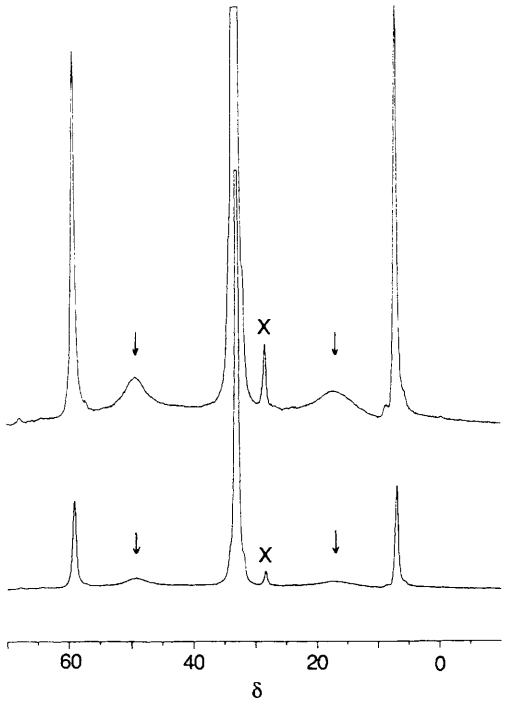

Fig. 5 The 121.47 MHz ^{31}P CP MAS NMR spectrum of $[HgI(NO_3)(PPh_3)]$; X = impurity, ↓ = peaks assigned as ^{201}Hg satellites (see text). The vertical scale of the upper trace is expanded (*ca.* ×4) relative to that of the lower trace

Solid-state ^{31}P *CP MAS NMR Spectra.*—There have been relatively few reports of solid-state ^{31}P CP MAS NMR spectra of complexes of mercury(II) with phosphine ligands.[24–27] Such studies are of potential value for establishing the relationship between the structures of such complexes in the solid state and in solution, since the NMR spectra can be obtained for both states, but detailed structural information is generally only available for solids. The solid-state ^{31}P CP MAS NMR spectrum of $[HgI(NO_3)(PPh_3)]$ is shown in Fig. 5; the spectra of the chloride and bromide complexes are similar. They each show a single central line due to species which contain the non-magnetic isotopes of Hg, together with satellites (with linewidths similar to that of the central line) which are assigned to $^1J(^{199}Hg^{31}P)$ coupling. The ^{31}P NMR parameters obtained from these spectra are listed in Table 6. The observation of single ^{31}P chemical shifts and coupling constants for each complex is consistent with the results of the crystal structure studies, which show that there is one molecule in each asymmetric unit and therefore only one phosphorus environment.

The ^{31}P NMR parameters measured for $[HgX(NO_3)(PPh_3)]$ in the solid state are compared with those observed for the corresponding complexes in MeCN solution in Table 6. The chemical shifts are not strongly dependent on X, but the variation with X is in opposite directions for the solution and solid samples, and there is a difference of about 10 ppm between the two sets of results. The $^1J(^{199}Hg^{31}P)$ values show opposite trends for the chloride (increasing from the solution to the solid state) relative to the bromide and iodide complexes (where a decrease is observed). This may be related to the difference in the crystal structure of the former complex compared with the latter (see above).

In addition to the sharp ^{199}Hg satellites which are also present in the solution spectra, the solid-state NMR spectra contain two much broader satellites (see peaks marked ↓ in Fig. 5). These appear reproducibly in different samples of the same complex, and their separation depends on X, being 5100, 4500, 3900 Hz (all ±100 Hz) for X = Cl, Br or I. These separations are 0.62 ± 0.01 times the $^1J(^{199}Hg^{31}P)$ coupling constants. Spectra measured at 161.90 MHz on the bromide and iodide complexes had the same appearance as those measured at 121.47 MHz, the frequency separations between the broad peaks remaining at the values listed above. The intensity of the satellites is approximately that expected from the natural abundance of ^{201}Hg (13.22% natural abundance, nuclear spin $I = \frac{3}{2}$), given the much greater linewidths of these peaks. Such lines have not been reported previously in similar studies of phosphine complexes of mercury(II).[24–27] The large nuclear quadrupole moment of ^{201}Hg and the asymmetric coordination environment in these complexes would be expected to give rise to rapid quadrupolar relaxation, so that any $^1J(^{201}Hg^{31}P)$ scalar coupling would be averaged to zero, and the signal due to species containing ^{201}Hg would occur in the central peak together with those of the species containing the non-magnetic isotopes of mercury, as is the case in solution. However, in some previously published solid-state ^{13}C CP MAS NMR studies of organomercury complexes it has been suggested that this might not be the case, and that the manner in which the ^{201}Hg species contribute to the spectrum has yet to be determined.[28,29]

The MAS NMR spectra of spin $I = \frac{1}{2}$ nuclei coupled to a quadrupolar nucleus have been discussed by various authors.[30–32] Menger and Veeman[30] have reported calculations of the line positions in terms of the various coupling constants involved. For the case where the spin $I = \frac{1}{2}$ nucleus is ^{31}P and the quadrupolar nucleus is a metal atom M, the relevant coupling constants are the metal nuclear Zeeman interaction $Z = \gamma_M hB/2\pi$, the metal nuclear quadrupole coupling constant $\chi = e^2qQ/h$, the phosphorus–metal dipolar coupling constant D [equation (2)] (r = the M–P bond length)

$$D = (\mu_0/4\pi)(\gamma_P\gamma_M/r^3)(h/4\pi^2) \quad (2)$$

and the indirect spin–spin coupling constant J. The form of the spectrum depends on the ratio $R = D/J$ of the dipolar to the indirect coupling constant and on the dimensionless parameter K [equation (3)] which is proportional to the ratio of the

$$K = -3\chi/4I(2I - 1)Z \quad (3)$$

copper quadrupole coupling constant to the copper nuclear Zeeman term. Menger and Veeman[30] have presented an analysis for three cases: where the spin $\frac{1}{2}$–spin $\frac{3}{2}$ interaction is purely dipolar, where it is purely scalar, and where mixed dipolar–scalar interactions exist. The results of this analysis are presented graphically in Figs. 3, 5 and 6 respectively of ref. 30. The most extensively studied case involves ^{31}P CP MAS NMR

Table 7 Comparison of ^1J(MP) from ^{31}P CP MAS NMR spectra of isostructural copper(I), silver(I), gold(I) and mercury(II) complexes with phosphorus-donor ligands

Complex	Metal nucleus M	Magnetogyric ratio, $\gamma/10^7$ T^{-1} s^{-1}	^1J(MP)/Hz	$10^6 J_r$[a]/T	Ref.
[CuCl{P[C$_6$H$_2$(OMe)$_3$-2,4,6]$_3$}]	^{63,65}Cu	7.247[b]	2040	28	31
[AgCl{P[C$_6$H$_2$(OMe)$_3$-2,4,6]$_3$}]	^{109}Ag	−1.250	785	63	34
[AuCl(PPh$_3$)]	^{197}Au	0.4625	520	112	*c*
[HgCl(PPh$_3$)]$^+$	^{199}Hg	4.815	8085	168	*c*

[a] $J_r = |J/\gamma|$. [b] The weighted mean of the values for the two isotopes was used in this case (see text). [c] This work.

spectra of compounds containing Cu–P bonds, where asymmetric quartets are normally observed due to coupling of ^{31}P to the quadrupolar ^{63,65}Cu nuclei ($I = \frac{3}{2}$). In this case R lies in the range 0.5–1.0 and K in the range 0–0.5 and the observed spectra correspond to the case shown in Fig. 6 of ref. 30.[30,33] In the case of the present mercury complexes, the $^1J(^{199}Hg^{31}P)$ coupling constants estimated from the corresponding $^1J(^{199}Hg^{31}P)$ coupling constants are 3000, 2700 and 2300 Hz for X = Cl, Br or I, respectively. The magnitude of the dipolar coupling constant D is estimated to be 270 Hz, so that $R \approx 0.1$, *i.e.* much smaller than for the ^{63,65}Cu–^{31}P case, and the situation corresponds more closely the case shown in Fig. 5 of ref. 30. The ^{201}Hg nuclear quadrupole coupling constants of the present complexes are not known, but can be estimated to be *ca.* 700 MHz from the ^{201}Hg $\nu(\frac{1}{2} \leftrightarrow \frac{3}{2})$ nuclear quadrupole resonance frequency in $HgCl_2$.[34] The ^{201}Hg Zeeman frequency at $B = 7.05$ T is 19.8 MHz, so that $K \approx 9$. Under these conditions the spectrum should consist of two lines symmetrically disposed about the position corresponding to the uncoupled ^{31}P signal, with a spacing of about 1.65 times the $^1J(^{201}Hg^{31}P)$ coupling constant.[30] Using the values of this coupling constant calculated from the observed $^1J(^{199}Hg^{31}P)$ coupling constants (see above) these spacings are estimated to be 5000, 4500 and 3800 Hz (X = Cl, Br or I) which agree within experimental error with the observed spacings between the broad signals assigned as ^{201}Hg satellites. This provides strong support for this assignment. The present system is a unique case with which to test the predicted form of the CP MAS NMR spectrum of a spin $\frac{1}{2}$ nucleus coupled to a quadrupolar nucleus, since the sample also contains non-quadrupolar isotopes ($I = 0, \frac{1}{2}$) of the quadrupolar nucleus which allow an accurate determination of the isotropic spin–spin coupling constant and the chemical shift.

The present results throw some light on the interpretation of the ^{31}P CP MAS NMR spectra of [AuX(PPh$_3$)] (X = Cl, Br or I).[5] These spectra consist of doublets, despite the fact that, like the mercury complexes in the present study, they contain only one crystallographic environment for the phosphorus atom. It was originally proposed that this splitting is due to inequivalence rather than to coupling.[5] However, a similar splitting was subsequently observed in some phosphole complexes of gold(I) halides,[35] and measurements over a wide range of field strengths (^{31}P frequencies from 60.75 to 145.75 MHz) show that the frequency separation in the doublet is field-independent,[36] suggesting that the splitting arises from coupling effects. Gold-197 (100% natural abundance, nuclear spin $I = \frac{3}{2}$) has a large quadrupole moment which is similar in magnitude to that of ^{201}Hg. The [HgX(NO$_3$)(PPh$_3$)] complexes contain quasi-linear [HgX(PPh$_3$)]$^+$ which are isoelectronic with [AuX(PPh$_3$)], so the bonding in these species should be quite similar. This suggests that the doublets observed in the spectra of the gold complexes are due to $^1J(^{197}Au^{31}P)$ coupling. The linewidths in these doublets are similar to those observed for the ^{201}Hg satellites of the [HgX(NO$_3$)(PPh$_3$)] complexes. The doublet splittings are 860, 830 and 680 Hz (X = Cl, Br or I),[5] and it is noteworthy that these splittings decrease from X = Cl to I by the same ratio as that of the $^1J(^{199}Hg^{31}P)$ values for [HgX(NO$_3$)(PPh$_3$)] [8085 Hz (Cl)/6330 Hz (I) = 1.3:1]. The ^{197}Au quadrupole coupling constant in [AuCl(PPh$_3$)] is χ = 940 MHz,[37] and the ^{197}Au Zeeman interaction at 7.05 T is Z = 5.14 MHz, so that $K \approx 45$ [equation (3)]. According to Fig. 5 of ref. 30, the spectrum should consist of two lines with a spacing of about 1.65 times the $^1J(^{197}Au^{31}P)$ coupling constant for $K > 10$. The resulting values of the $^1J(^{197}Au^{31}P)$ coupling constants calculated from the observed spacings of the doublets are 520, 500 and 410 Hz (X = Cl, Br or I). The dipolar coupling constant for these complexes is D = 60 Hz [equation (2)], so that $R = D/J \approx 0.1$, *i.e.* the same as for the mercury complexes. It is therefore consistent to use the same analysis for both sets of complexes.

In order to determine whether the $^1J(^{197}Au^{31}P)$ values estimated in this way are reasonable, the result for the X = Cl case is compared in Table 7 with those for other ^1J(MP) values for systems involving linear two-co-ordinate P–M–Cl entities. For the M = Cu or Ag cases, linear two-co-ordinate [MCl(L)] complexes do not exist for L = PPh$_3$, but such complexes have been characterized with the more sterically demanding ligand L = tris(2,4,6-trimethoxyphenyl)phosphine.[33,38] In order to eliminate the effect of the different magnetic moments of the metal nuclei on these coupling constants, these constants have been divided by the magnetogyric ratio γ of the metal nucleus concerned (the value used for the copper nucleus is the weighted mean of those for the naturally occurring isotopes ^{63}Cu and ^{65}Cu since separate signals for the two isotopes were not resolved in this case). This yields a reduced coupling constant J_r which is essentially the magnitude of the magnetic field at the metal nucleus which is induced by the magnetic moment of the phosphorus nucleus by means of the Fermi contact interaction between the nuclei and the electrons in the M–P bond. Since this arises from the Fermi contact interaction it depends on the contributions of the phosphorus and the metal valence s orbitals to the M–P bonds. The complexes which are compared in Table 7 have similar phosphorus-donor ligands, so the phosphorus s orbital contribution should be similar in all cases. Thus, the values of J_r should be a reflection of the metal valence s-orbital contribution to the M–P bond. The results in Table 7 show that the J_r values for the silver complexes are about a factor of 2 greater than those of the corresponding copper complexes, an observation which has been made previously for a range of other isostructural complexes of Cu and Ag.[39] It now appears that this quantity increases by a further factor of 2 from Ag to Au. There is a smaller increase from Au to Hg, but the values are of similar magnitude, as would be expected for these isoelectronic species. Thus, this comparison suggests that the $^1J(^{197}Au^{31}P)$ values which result from the above analysis are of reasonable magnitude. They should, however, be regarded as very approximate at this stage. Further work is required to investigate the effects on the spectra of changes in the experimental conditions under which the spectra are obtained, and to explain why the effect is only observed in linear or nearly linear complexes with certain combinations of ligands.

Acknowledgements

We acknowledge support of this work by grants from the New Zealand University Grants Committee, the University of Auckland Research Committee, and the Australian Research Grants Scheme. We thank Dr. John Seakins for recording the Raman spectra, Dr. Michael Liddell for running the solution ^{31}P NMR spectra, David Camp and Kerry Penman of the Brisbane NMR Centre for recording the CP MAS NMR spectra, and Dr. Peter Meier of Varian, Darmstadt, for obtaining CP MAS spectra on the Unity 400 spectrometer.

References

1 P. L. Goggin, R. J. Goodfellow, S. R. Haddock and J. G. Eary, *J. Chem. Soc., Dalton Trans.*, 1972, 647.
2 P. L. Goggin, R. J. Goodfellow, D. M. McEwan, A. J. Griffiths and K. Kessler, *J. Chem. Res.*, 1979, (*S*) 194.
3 G. A. Bowmaker and D. A. Rogers, *J. Chem. Res.*, 1988, (*S*) 2825; 1984, (*M*) 1601.
4 T. S. Lobana, M. K. Sandhu, D. C. Povey and G. W. Smith, *J. Chem. Soc., Dalton Trans.*, 1988, 2913.
5 P. F. Barron, L. M. Engelhardt, P. C. Healy, J. Oddy and A. H. White, *Aust. J. Chem.*, 1987, **40**, 1545.
6 J. A. Ibers and W. C. Hamilton (Editors), *International Tables for X-Ray Crystallography*, Kynoch Press, Birmingham, 1974, vol. 4.
7 S. R. Hall and J. M. Stewart (Editors), *XTAL Users' Manual, Version 3.0*, Universities of Western Australia and Maryland, 1990.
8 F. A. Cotton and G. Wilkinson, *Advanced Inorganic Chemistry*, 5th edn., Wiley, New York, 1988.
9 K. Köhler, D. Breitinger and G. Thiele, *Angew. Chem., Int. Ed. Engl.*, 1974, **13**, 821.
10 J. V. Hatton, W. G. Schneiderr and W. Siebrand, *J. Chem. Phys.*, 1963, **39**, 1330; P. G. Jones, *Gold Bull.*, 1981, **14**, 102 and refs. therein.
11 N. A. Bell, M. Goldstein, T. Jones and I. W. Nowell, *Inorg. Chim. Acta*, 1980, **43**, 87.
12 N. A. Bell, L. A. March and I. W. Nowell, *Inorg. Chim. Acta*, 1989, **156**, 201.
13 N. A. Bell, T. D. Dee, M. Goldstein, P. J. McKenna and I. W. Nowell, *Inorg. Chim. Acta*, 1983, **71**, 135.
14 L. Fälth, *Chem. Scr.*, 1976, **9**, 71.
15 N. A. Bell, M. Goldstein, T. Jones and I. W. Nowell, *Inorg. Chim. Acta*, 1983, **69**, 155.
16 G. B. Deacon, J. H. S. Green and D. Harrison, *Spectrochim. Acta, Part A*, 1968, **24**, 1921.
17 D. R. Williamson and M. C. Baird, *J. Inorg. Nucl. Chem.*, 1972, **34**, 3393.
18 L. V. Konovalov and K. A. Davarski, *J. Coord. Chem.*, 1986, **14**, 201.
19 N. A. Bell, M. Goldstein, T. Jones and L. A. March, *Inorg. Chim. Acta*, 1982, **61**, 83.
20 A. G. Jones and D. B. Powell, *Spectrochim. Acta, Part A*, 1974, **30**, 563.
21 K. Nakamoto, *Infrared and Raman Spectra of Inorganic and Coordination Compounds*, 4th edn., Wiley, New York, 1986.
22 C. C. Addison, N. Logan, S. C. Wallwork and C. D. Garner, *Q. Rev. Chem. Soc.*, 1971, **25**, 289.
23 L. I. Katzin, *J. Inorg. Nucl. Chem.*, 1962, **24**, 245.
24 T. Allman, F. Bélanger-Gariépy and A. L. Beauchamp, *J. Crystallogr. Spectrosc. Res.*, 1990, **20**, 149.
25 E. C. Alyea, K. J. Fisher and S. Johnson, *Can. J. Chem.*, 1989, **67**, 1319.
26 T. Allman, *J. Magn. Reson.*, 1989, **83**, 637.
27 T. Allman and R. E. Lenkinski, *Inorg. Chem.*, 1986, **25**, 3202.
28 A. M. Hounslow, S. F. Lincoln and E. R. T. Tiekink, *J. Organomet. Chem.*, 1988, **354**, C9.
29 R. D. Kendrick, C. S. Yannoni, R. Aikman and R. J. Lagow, *J. Magn. Reson.*, 1980, **37**, 555.
30 E. M. Menger and W. S. Veeman, *J. Magn. Reson.*, 1982, **46**, 257.
31 J. Bohm, D. Fenzke and H. Pfeifer, *J. Magn. Reson.*, 1983, **55**, 197.
32 R. K. Harris, *J. Magn. Reson.*, 1988, **78**, 389.
33 G. A. Bowmaker, J. D. Cotton, P. C. Healy, J. D. Kildea, S. B. Silong, B. W. Skelton and A. H. White, *Inorg. Chem.*, 1989, **28**, 1462.
34 D. B. Patterson, G. E. Peterson and A. Carnevale, *Inorg. Chem.*, 1973, **12**, 1283.
35 S. Attar, W. H. Bearden, N. W. Alcock, E. C. Alyea and J. H. Nelson, *Inorg. Chem.*, 1990, **29**, 425.
36 J. H. Nelson, personal communication.
37 P. G. Jones, A. G. Maddock, M. J. Mays, M. M. Muir and A. F. Williams, *J. Chem. Soc., Dalton Trans.*, 1977, 1434.
38 L.-J. Baker, G. A. Bowmaker, D. Camp, Effendy, P. C. Healy, H. Schmidbaur, B. W. Skelton, O. Steigelmann and A. H. White, unpublished work.
39 S. Attar, N. W. Alcock, G. A. Bowmaker, J. S. Frye, W. H. Bearden and J. H. Nelson, *Inorg. Chem.*, 1991, **30**, 4166.

Received 25*th October* 1991; *Paper* 1/05446E